NASA Technical Memorandum 86978

Experimental Stiffness of Tapered Bore Seals

David P. Fleming
Lewis Research Center
Cleveland, Ohio

Prepared for the
Design Engineering Technical Conference
sponsored by the American Society of Mechanical Engineers
Cincinnati, Ohio, September 10–13, 1985

NASA

EXPERIMENTAL STIFFNESS OF TAPERED BORE SEALS

David P. Fleming
National Aeronautics and Space Administration
Lewis Research Center
Cleveland, Ohio 44135

ABSTRACT

The stiffness of tapered-bore ring seals was measured with air as the sealed fluid. Static stiffness agreed fairly well with results of a previous analysis. Cross-coupled stiffness due to shaft rotation was much less than predicted. Part of the disparity may be due to simplifying assumptions in the analysis; however, these do not appear to account for the entire difference observed.

INTRODUCTION

Analyses have shown that annular pressure seals (ring seals) can generate significant lateral forces. Those papers included as references [1-5, 8-10] are but representative of the attention these seals have received from rotordynamicists in recent years. Analysts have also predicted that tapered-bore seals will be significantly stiffer than straight-bore seals [2]. Experiments for tapered-bore seals with a liquid fluid have shown reasonable agreement between theory and experiment [4]. Extremely limited experimental results have been published for forces in seals flowing compressible fluids. These are in [5], in which the only seal positions tested were concentric and fully eccentric; seal forces were inferred from pressure measurements at only a few circumferential locations.

Tapered bore seals have been used successfully where straight-bore seals were unsuccessful. One such application was the hot gas seal in the space shuttle high-pressure oxygen pump. This is a floating ring seal. The low centering forces developed by the straight-bore seal allowed rubbing to occur

as the seal attempted to follow shaft excursions; this resulted in rapid seal wear. The higher film force of the tapered-bore seal permitted the seal to follow the shaft motions without rubbing, hence eliminating wear.

The purpose of the present work is to measure the load-deflection characteristics of tapered-bore seals with air as the sealed fluid. Further, the experimental data will be compared with the analytical predictions of [2].

NOMENCLATURE

B	seal damping coefficient
C_1, C_2	entrance and exit radial clearance for concentric seal
D	seal diameter
e	eccentricity
F_x, F_y	seal force in x and y directions
f	friction factor
K	seal direct stiffness coefficient
R	dimensionless stiffness, KC_2/p_oLD
k	cross-coupled stiffness coefficient
L	seal length
P_o, P_3	reservoir and sump pressures
R	seal radius
W	total load on seal
w	circumferential velocity component
x,y	transverse coordinates
z	axial coordinate
ϵ	eccentricity ratio, e/C_2
σ	dimensionless friction factor, fL/C_2
ϕ	attitude angle
ω	rotational speed

APPARATUS

The test apparatus was originally designed for use with herringbone-grooved journal bearings; its description for that use appears in [6] and [7]. For the present work, the hydrodynamic bearing sleeves were replaced by the tapered-bore seals shown in Fig. 1. Air is supplied to the center of the seal and flows out at each end. The overall apparatus is shown in Fig. 2. The apparatus was further modified by provision of air supply passages to the center section of each seal pair and by pressure taps for measurement of the pressure at the seal entrance (Fig. 2). This pressure measurement was made in the annulus on the outer diameter of the seal insert (Fig. 1); it was assumed that air velocity in this annulus and pressure drop from the annulus to the seal entrance were negligible. The herringbone-grooved shafts of [6] and [7] were replaced by smooth shafts having provision for balancing screws at each end. Several shafts were made with varying diameters. The seals are 38 mm in diameter and 17.5 mm long; this results in a length-to-diameter ratio of 0.46.

Radial loads in an upward direction (along the y-axis) were applied to the shaft by a rolling-diaphragm air cylinder acting through an externally-pressurized load shoe. For those tests in which shaft rotation was desired, the shaft was driven by an impulse turbine. This consists of 12 buckets cut into the shaft at one end; the shaft is surrounded by a nozzle ring. A magnetic pickup adjacent to the turbine buckets is connected to a speed controller and to a digital counter for speed measurement.

Two orthogonally-oriented capacitance distance probes are mounted outboard of each seal pair. They were used to measure the displacement of the shaft under load, and also the assembled clearance of the shaft in the seals. Because of slight misalignment of the two seals, the apparent assembled

clearance (as measured by the capacitance probes) was 0.001 mm less than the nominal clearance.

The load cylinder had been previously calibrated to determine the relationship between cylinder pressure and applied force. During test runs the pressure was measured with a transducer whose output was transmitted to a modular instrument computer (MINC). The capacitance probe output was also transmitted to the MINC. These data were read under the control of a FORTRAN computer program, which then provided near-instantaneous reduction of the raw data. The MINC also graphed the results: an example of graphical output appears as Fig. 3. The output variable was seal stiffness; in dimensional terms this is defined as the applied force divided by the shaft displacement.

EXPERIMENTAL PROCEDURE

The air pressure to the seals was set at the desired value. Usually one seal required a higher pressure than the other (due to minor geometric differences) in order that the displacement under load be the same for both seals. This difference in required pressure was assumed to be due to slight (unintentional) variations in seal geometry and alignment. The loader pressure was set so the applied upward force just balanced the weight of the shaft. The resulting shaft position was recorded and all subsequent shaft motion referenced to this zero-net-load position. Shaft speed was then set and load increased in small increments to some maximum value. This value was chosen to cause contact between shaft and seals when the shaft was stationary, and to maintain some small clearance when the shaft was rotating. After reaching the maximum value, the load was decreased in increments to the zero-net-load value. Seal leakage was not measured.

RESULTS

Shafts of three different diameters were used in a single set of seals. Table 1 shows the resulting clearances and clearance ratios obtained.

Figure 3 is representative of the load versus eccentricity data obtained and plotted by the MINC. The load has been nondimensionalized and given the form of a stiffness. This stiffness is very nearly constant out to an eccentricity ratio of 0.6. Thus one can conclude that small eccentricity analysis is adequate for eccentricity ratios of 0.6 or less. The analysis of [8], for incompressible fluids in straight seals, reaches similar conclusions. Figure 3 uses different plot symbols for increasing and decreasing loads; consistency between the two sets of data was a requisite for acceptability of the data.

The small-eccentricity values of seal stiffness for a number of data runs have been plotted as a function of seal pressure ratio in Figs. 4 to 6. Also plotted are calculated stiffness values from the analysis of [2].

The shape of the analytical curves in some cases appears peculiar at first glance. It is due to the nature of the flow changing with pressure ratio. This may be explained with reference to Fig. 4. For low pressure ratios, the flow is both laminar and unchoked. As pressure ratio rises, the seal exit Mach number also rises, until fluid exit velocity becomes sonic at a pressure ratio just over four. This change from an unchoked to a choked condition produces the discontinuity in the slope of the curve at that point. The flow remains laminar up to a pressure ratio of about 4.9 when the critical Reynolds number of 2300 is reached (using twice the clearance as the significant length in forming the Reynolds number). For higher pressure ratios, the flow then becomes turbulent, with an increase in friction factor. This change produces a discontinuity in the stiffness curve at this point. Between Reynolds numbers of 2300 and 3000 there is uncertainty as to whether the flow is laminar or turbulent. The stiffness curve between the pressure ratios corresponding to these Reynolds numbers has therefore been indicated by a straight dashed line.

The trends of the data appear to be well predicted by the analysis. The magnitude of the stiffness is not always predicted accurately, however. The disparity is greatest for the smallest seal clearance (0.010 mm), with predicted values being some 30 percent greater than measured. For the 0.023 cm clearance, measured and predicted values are within about 10 percent of each other and for the 0.037 mm clearance the agreement is excellent.

Part of the disparity could be due to the one-dimensional analysis used. That is, circumferential flow of the fluid has been neglected. Circumferential flow would assume more significance at larger values of clearance ratio; this is the case for the 0.010 mm clearance seal where the inlet (concentric) clearance is over three times the exit clearance. An analysis is reported in [3] which accounts for circumferential flow. Unfortunately, results of this analysis are only available for turbulent flow cases.

Measured stiffness could also be different than predicted because of the slight misalignment of the seals. As mentioned above, the apparent clearance of the assembly (as measured by the capacitance probes) was some 0.001 mm less than the difference between measured seal and shaft radii. Misalignment would be expected to reduce the seal stiffness. The effect would be greatest for the seals with smallest clearance, as the relative change in clearance is greatest for this case. Results could also be affected by measurement errors. Most significant is the error in measuring seal clearance which could be as much as 0.002 mm. This maximum probable error is 20 percent of the smallest clearance tested and would produce a change of 20 percent in dimensionless stiffness. If in the right direction this could reduce by more than half the disparity between measured and calculated values in Fig. 6.

Effect of Seal Rotation

Analyses predict changes in seal behavior from rotational effects. From Ref. 9, for steady state conditions, seal forces are given by

$$\begin{bmatrix} F_x \\ F_y \end{bmatrix} = -\begin{bmatrix} K & B\omega/2 \\ -B\omega/2 & K \end{bmatrix} \begin{bmatrix} x \\ y \end{bmatrix} \tag{1}$$

The off-diagonal terms in the matrix are known as cross-coupled stiffness and are related to the seal damping as shown when circumferential fluid velocity equals $R\omega/2$ throughout the seal. In the test setup the load is applied in the y direction; thus $F_x = 0$, and x may be expressed as

$$x = -B\omega y/2K \tag{2}$$

and

$$W = F_y = -Ky[(B\omega/2K)^2 + 1] \tag{3}$$

Radial displacement (eccentricity) e is

$$e = (x^2 + y^2)^{1/2} = y[(B\omega/2K)^2 + 1]^{1/2} \tag{4}$$

The apparent seal stiffness is

$$K_{app} = -W/e = K[B\omega/2K)^2 + 1]^{1/2} \tag{5}$$

Shaft displacement will not be colinear with the load but at an attitude angle given by

$$\phi = \tan^{-1}(-x/y) = \tan^{-1}(B\omega/2K) \tag{6}$$

The present experimental setup did not allow the direct measurement of seal damping. However, as Eqs. (5) and (6) indicate, the presence of damping will affect the measured stiffness and attitude angle. Analytical values of stiffness and damping, from [2] and [9] may be used to calculate the expected effects of rotation. At the test speeds one would expect stiffness increases of 15 to 34 percent compared to the static case, and attitude angles of 29 to 42 degrees.

Such changes were not observed. Figure 7, for shaft 3 at 20 000 rpm, shows no significant change from Fig. 3, the static case. Stiffness data for other shafts and pressures also showed no clear effects of rotation. Attitude angles were much lower than predicted. Table 2 summarizes the results obtained.

Two possibilities were explored as reasons for the disparity between analysis and experiment. These were development of the circumferential flow field and the limitations of the one-dimensional analysis.

Equation (1) assumes developed circumferential flow throughout the seal. In the experiments no attempt was made to impart circumferential velocity (or preswirl) to the fluid entering the seal. Therefore, there is some length over which the circumferential velocity changes from the entrance value to the fully developed value. As pointed out in [10], the cross-coupled stiffness will be less than that shown in Eq. (1) when the average circumferential velocity is less than $R\omega/2$. For a straight-bore seal with incompressible fluid and no initial swirl, circumferential velocity development was derived in [10]

$$w = R\omega(1-e^{-\sigma z/L})/2 \qquad (7)$$

An entrance length may be defined as the distance from the seal entrance at which the circumferential velocity reaches 95 percent of its fully-developed value. For the conditions producing the data of Fig. 7, using the average clearance in the seal, the entrance length is 35 percent of the total seal length. Thus circumferential flow is fully developed over the majority of the seal. It may be noted that Fig. 7 is for the largest seal clearance tested; smaller clearances are associated with shorter entrance lengths.

The present test configuration (compressible fluid and tapered-bore seal) differs from the configuration for which Eq. (7) was derived. Nevertheless,

it seems unlikely that circumferential flow development is entirely responsible for the large difference between analysis and experiment.

The analyses of [2] and [9] are for one-dimensional flow. That is, pressure-induced circumferential flow is neglected. This is another possible source of inaccuracy. In [3], this restrictive assumption is not made. As previously mentioned, results from [3] are available only for turbulent flow; the present test data is nearly all for laminar flow conditions. However, it was believed worthwhile to compare published results of [3] with those of [2] and [9]. The seal for which results are shown in Table 4 of [3] is closest to the present seals; the geometric configuration is similar but flow is turbulent. Table 3 shows the seal operating conditions and Table 4 the results from [3] as well as results for this configuration from the analyses of [2] and [9].

The two analyses agree fairly well for direct stiffness. For both damping and cross-coupled stiffness, however, the more sophisticated analysis of [3] predicts considerably lower coefficients than the analyses of [2] and [9]. It may be that if the analysis of [3] were extended to the laminar flow case that similarly lower coefficients would be predicted. Until the work is done, however, this is conjecture. Thus definite conclusions regarding the present correlation must await further analytical development.

SUMMARY OF RESULTS

Experiments were performed to measure the stiffness of tapered-bore ring seals with air as the sealed fluid; flow through the seals was laminar. Seals with three different clearances and clearance ratios (inlet clearance/outlet clearance) were tested. Static stiffness agreed fairly well with results of a previous analysis; agreement was best for the largest-clearance seal tested. Cross-coupled stiffness due to shaft rotation was much less than predicted.

Part of the disparity may be due to simplifying assumptions in the analysis; however, these do not appear to account for the entire difference observed.

REFERENCES

1. Black, H.F., "Effects of Hydraulic Forces in Annular Pressure Seals on the Vibrations of Centrifugal Pump Rotors," Journal of Mechanical Engineering Science, Vol. 11, No. 2, Apr. 1969, pp. 206-213.
2. Fleming, David P, "Stiffness of Straight and Tapered Annular Gas Path Seals," Journal of Lubrication Technology, Vol. 101, No. 3, July 1979, pp. 349-355.
3. Nelson, C.C., "Rotordynamic Coefficients for Compressible Flow in Tapered Annular Seals," (to be published in Journal of Tribology.)
4. Childs, D.W., and Dressman, John B., "Convergent-Tapered Annular Seals: Analysis and Testing for Rotordynamic Coefficients," ASME Paper 84-Trib-33 (to be published in Journal of Tribology.)
5. Hendricks, R.C., "Some Flow Characteristics of Conventional and Tapered High-Pressure-Drop Simulated Seals," ASLE Transactions, Vol. 24, No. 1, Jan. 1981, pp. 23-28.
6. Cunningham, R.E., Fleming, D.P., and Anderson, W.J., "Experimental Stability Studies of the Herringbone-Grooved Gas-Lubricated Journal Bearing," Journal of Lubrication Technology, Vol. 91, No. 1, Jan. 1969, pp. 52-59.
7. Cunningham, R.E., Fleming, D.P., and Anderson, W.J., "Experimental Load Capacity and Power Loss of Herringbone Grooved Gas Lubricated Journal Bearings," Journal of Lubrication Technology, Vol. 93, No. 3, July 1971, pp. 415-422.

8. Allaire, P.E., Lee, C.C., and Gunter, E.J., "Dynamics of Short Eccentric Plain Seals with High Axial Reynolds Numbers," Journal of Spacecraft, Vol. 15, No. 6, Nov.-Dec. 1978, pp. 341-347.

9. Fleming, David P., "Damping in Ring Seals for Compressible Fluids," Rotordynamic Instability Problems in High Speed Turbomachinery, NASA CP-2133, 1980, pp. 169-188.

10. Black, H.F., Allaire, P.E., and Barrett, L.E., "Inlet Flow Swirl in Short Turbulent Annular Seal Dynamics," Papers Presented at the Ninth International Conference on Fluid Sealing, BHRA Fluid Engineering, Cranfield, England, 1981, pp. 141-152.

TABLE 1. - SEAL CLEARANCES AND CLEARANCE RATIOS

Shaft	Outlet clearance, mm	Inlet clearance/ outlet clearance
1	0.010	3.1
2	.023	1.9
3	.037	1.5

TABLE 2. - ROTATIONAL EFFECTS IN SEALS

Shaft	Speed, rpm	Pressure ratio	Attitude angle, degree		Stiffness increase, percent*	
			Measured	Calculated	Measured	Calculated
1	18 000	5.2	17	42	0	34
2	30 000	6.5	18	34	7	20
3	20 000	3.1	7	29	0	15

*Compared to static case.

TABLE 3. - SEAL CONDITIONS FOR ANALYSIS COMPARISON

Reservoir pressure, p_0, MPa	1.52
Sump pressure, p_3, MPa	0.65
Reservoir temperature, K	650
Fluid viscosity, μPa s	18
Fluid gas constant, J/kg K	2590
Seal length, L, mm	26
Seal radius, R, mm	32.5
Entrance clearance, C_1, mm	0.172
Exit clearance C_2, mm	0.086
Rotational speed, rpm	30 400

TABLE 4. - STIFFNESS AND DAMPING IN TURBULENT TAPERED-BORE SEAL

	Direct stiffness, kN/m	Cross-coupled stiffness, kN/m	Attitude angle, degree	Direct damping, Ns/m
Nelson [3]	2880	267	5.3	152
Fleming [2, 9]	3316	495	8.5	311

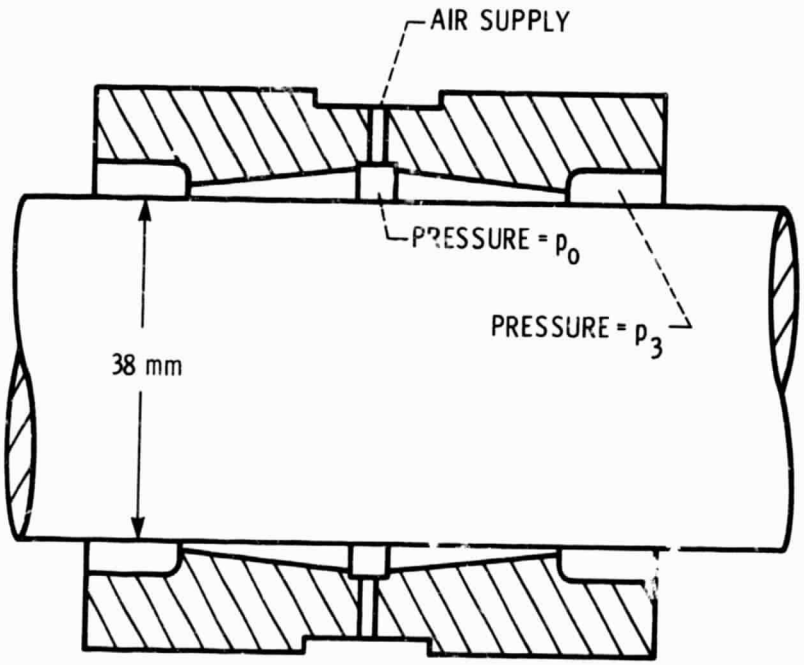

Figure 1. - Tapered bore seal.

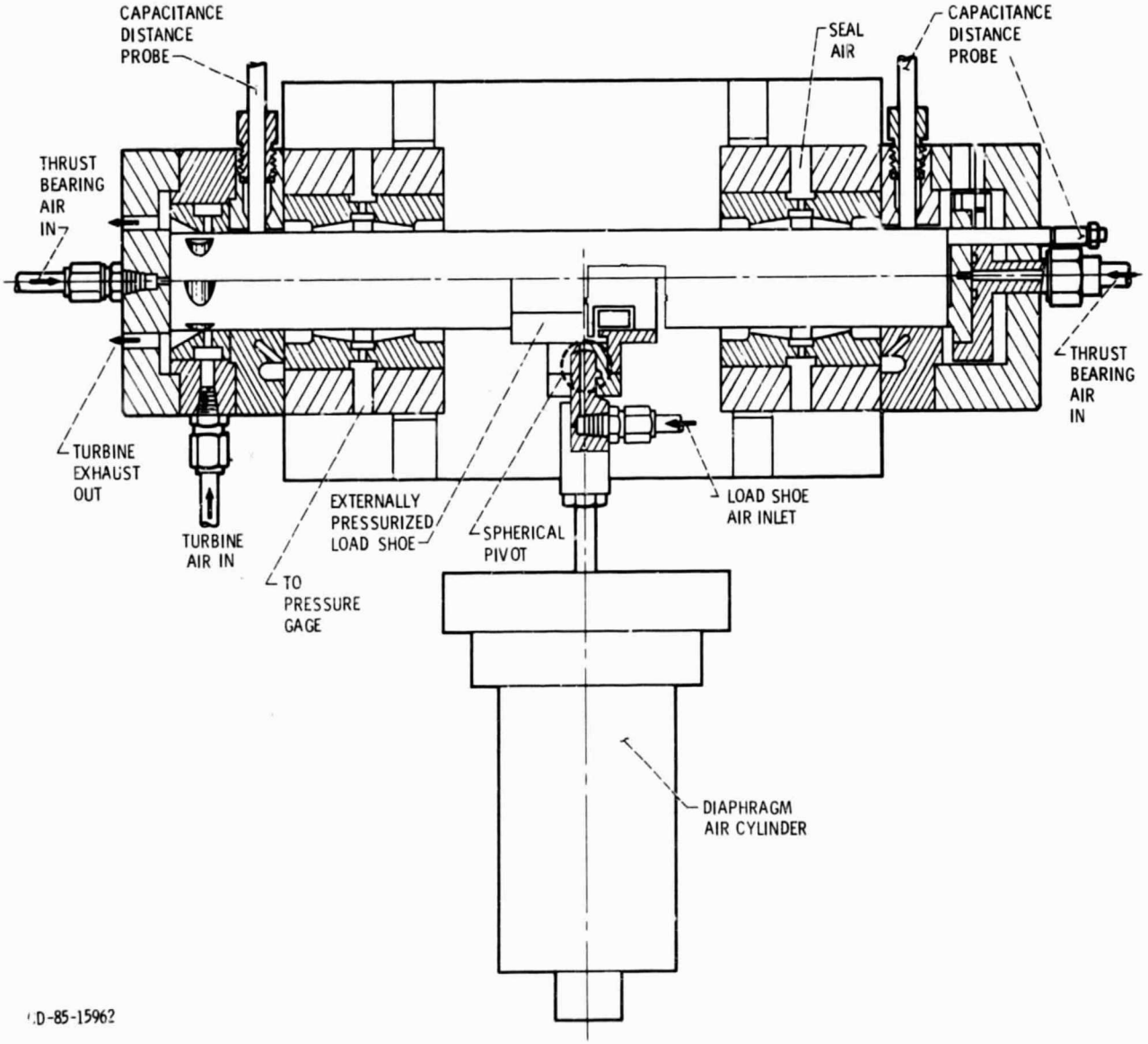

CD-85-15962

Figure 2. - Test apparatus.

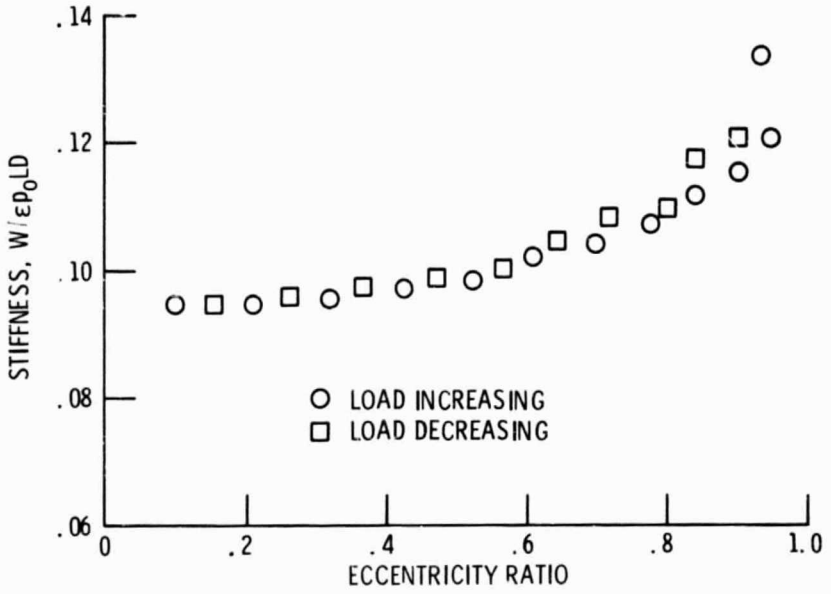

Figure 3. - Load-eccentricity data: clearance, 0.037 mm; pressure ratio, 3.1; no rotation.

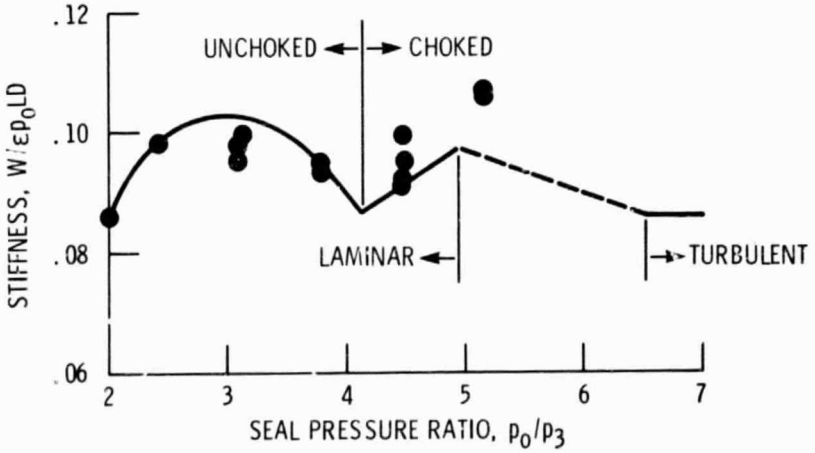

Figure 4. - Small eccentricity stiffness: clearance, 0.037 mm; no rotation.

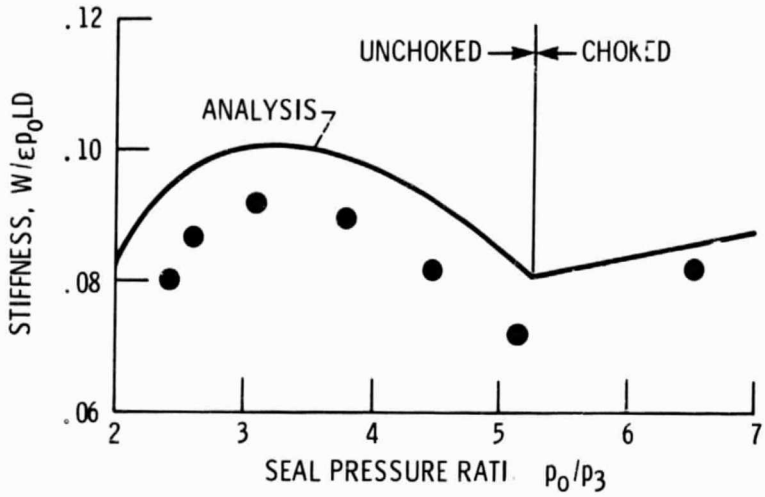

Figure 5. - Small eccentricity stiffness: clearance, 0.023 mm; no rotation.

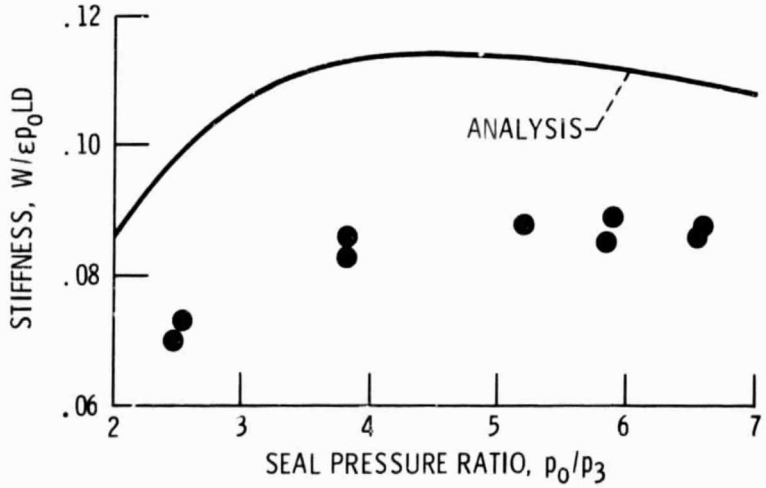

Figure 6. - Small eccentricity stiffness: clearance, 0.010 mm; no rotation.

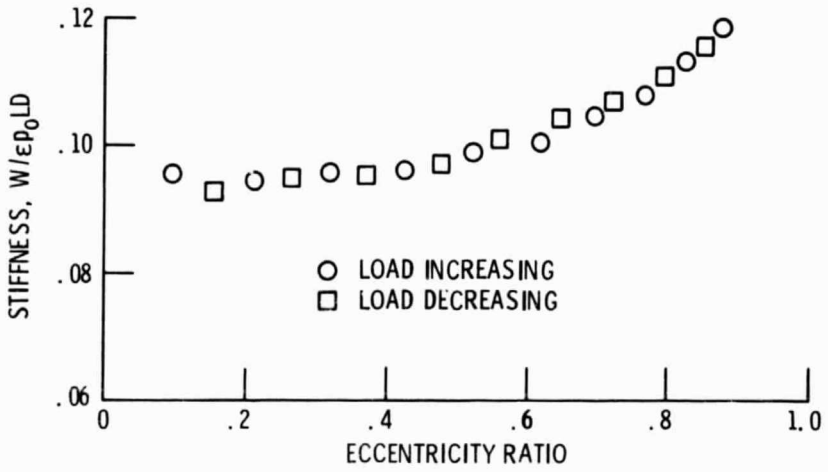

Figure 7. - Load-eccentricity data: clearance, 0.037 mm; pressure ratio, 3.1; speed, 20 000 rpm.

1. Report No.	2. Government Accession No.	3. Recipient's Catalog No.
NASA TM-86978		

4. Title and Subtitle	5. Report Date
Experimental Stiffness of Tapered Bore Seals	
	6. Performing Organization Code: 505-33-7B

7. Author(s)	8. Performing Organization Report No.
David P. Fleming	E-2515
	10. Work Unit No.

9. Performing Organization Name and Address	11. Contract or Grant No.
National Aeronautics and Space Administration Lewis Research Center Cleveland, Ohio 44135	
	13. Type of Report and Period Covered: Technical Memorandum
12. Sponsoring Agency Name and Address	
National Aeronautics and Space Administration Washington, D.C. 20546	14. Sponsoring Agency Code

15. Supplementary Notes

Prepared for the Design Engineering Technical Conference sponsored by the American Society of Mechanical Engineers, Cincinnati, Ohio, September 10-13, 1985.

16. Abstract

The stiffness of tapered-bore ring seals was measured with air as the sealed fluid. Static stiffness agreed fairly well with results of a previous analysis. Cross-coupled stiffness due to shaft rotation was much less than predicted. Part of the disparity may be due to simplifying assumptions in the analysis; however, these do not appear to account for the entire difference observed.

17. Key Words (Suggested by Author(s))	18. Distribution Statement
Ring seals Seal forces	Unclassified - unlimited STAR Category 37

19. Security Classif. (of this report)	20. Security Classif. (of this page)	21. No. of pages	22. Price*
Unclassified	Unclassified		

*For sale by the National Technical Information Service, Springfield, Virginia 22161